

Oversampled Deadbeat Current Control Strategy for PMSM Drives

Luca Rovere, Andrea Formentini, Pericle Zanchetta

Department of Electrical and Electronic Engineering, The University of Nottingham
Nottingham, NG7 2RD, U.K.

luca.rovere@nottingham.ac.uk , andrea.formentini@nottingham.ac.uk, pericle.zanchetta@nottingham.ac.uk

Abstract—This paper presents a novel deadbeat current control approach for Permanent Magnet Synchronous Motors (PMSMs) drives capable of operating at a controller sampling frequency multiple of the power converter switching frequency. The proposed technique permits to achieve a constant switching frequency and an optimal current ripple along with a high current loop bandwidth and robust behaviour to parameter variation.

Keywords—Deadbeat Control, PMSM Drives

I. INTRODUCTION

PMSMs offer different advantages in the field of variable-speed AC drives compared to other motor types such as induction motors. They present higher efficiency, higher performance, compact construction, higher torque per volume ratio. Recently the trend towards a fully digital control of power converters based on deadbeat current control is increasing [1-3]. This technique permits to achieve a fast transient response, precise current control and it is fully compatible with digital control platforms. The deadbeat control in combination with the space vector modulation (SVM) technique is able to provide the lowest distortion and the lowest current ripples [4]. In the attempt of pushing the system dynamic performance without increasing the converter switching frequency and/or using expensive new Wide Band Gap (WBG) devices, another emerging model based control technique, Finite Control Set Model Predictive Control (FCS-MPC) [5-8], has received in recent years a great interest from the academic community. It uses the model of the system to predict its future states for every possible control action. The best control action is then chosen by minimizing a cost function. This approach does not require a modulator, reduces the control sample time and decreases consequently the response time. These features lead to high bandwidth in the dynamic response and robust behaviour to parameter variation and system imperfection. On the other hand however, the absence of a modulator results in a variable switching frequency that usually results in a suboptimal current ripple. This paper investigates a new dead beat approach in order to operate at an increased controller sampling frequency without increasing the commutation frequency of the power converter. The proposed technique permits to achieve a constant switching frequency and an optimal current ripple along with a

high current loop bandwidth and robust behaviour to parameter variation.

The system configuration studied here is composed by a DC voltage source that supplies a three phase two levels Voltage Source Inverter (VSI) which is connected to a PMSM. The proposed new deadbeat current controller generates the phase voltage control references which are fed into a Pulse Width Modulator (PWM) that gives as output the gate signals to control the VSI IGBTs. The new oversampled deadbeat controller is obtained by discretizing the system equations over a variable sample time T_{s_i} resulting in an increased control sampling frequency. Although the proposed oversampling approach increase the robustness to machine parameters variation, on the other hand it introduces a distortion in the control voltages fed into the PWM, causing an offset in the controlled PMSM currents. To eliminate this behaviour a compensation strategy has been developed and successfully validated. Simulations have been carried out with successful results regarding the robustness achieved with the oversampling algorithm and the elimination of the control offset with the control voltage compensation. Furthermore increased performance at speed higher than 3000 rpm, consisting in the phase current Total Harmonic Distortion (THD) reduction, has been noticed with the compensation proposed.

II. PMSM MODEL AND DEADBEAT CONTROL

The mathematical model of a PMSM in rotor synchronous reference frame qd is reported in (1):

$$\begin{bmatrix} V_{qs} \\ V_{ds} \end{bmatrix} = \begin{bmatrix} R_s & 0 \\ 0 & R_s \end{bmatrix} \begin{bmatrix} i_{qs} \\ i_{ds} \end{bmatrix} + \begin{bmatrix} p & \omega_r \\ -\omega_r & p \end{bmatrix} \begin{bmatrix} \lambda_{qs} \\ \lambda_{ds} \end{bmatrix} \quad (1)$$

where V_{qs} , V_{ds} , λ_{qs} , λ_{ds} and i_{qs} , i_{ds} are the stator q- and d-axes voltage, flux linkage, and current in the rotor reference frame, R_s is the stator resistance, ω_r is the rotor angular velocity, and p is the derivative operator. The stator flux linkage viewed in a rotor synchronous reference frame is given by (2):

$$\begin{bmatrix} \lambda_{qs} \\ \lambda_{ds} \end{bmatrix} = [L_{ss}^{qd}] \begin{bmatrix} i_{qs} \\ i_{ds} \end{bmatrix} + [\lambda_m^{qd}] \quad (2)$$

where

$$\begin{bmatrix} L_{qs} \\ L_{ds} \end{bmatrix} = \begin{bmatrix} L_q & 0 \\ 0 & L_d \end{bmatrix} \quad \begin{bmatrix} \lambda_m^{qd} \\ \lambda_m^{dq} \end{bmatrix} = \lambda_m \begin{bmatrix} 0 \\ 1 \end{bmatrix} \quad (3)$$

L_q, L_d are q- axis and d-axis inductance in the rotor reference frame, λ_m is the peak flux linkage established by the magnets. The model in (1) has been discretized using the Euler discretization method for digital implementation. The discretization around a generic time instant k leads to the following equations:

$$\begin{bmatrix} i_{qs\ k+1} \\ i_{ds\ k+1} \end{bmatrix} = A \begin{bmatrix} i_{qs\ k} \\ i_{ds\ k} \end{bmatrix} + B_1 \begin{bmatrix} V_{qs\ k} \\ V_{ds\ k} \end{bmatrix} + B_2 \begin{bmatrix} \lambda_m \\ 0 \end{bmatrix} \quad (4)$$

$$A = \begin{bmatrix} 1 - \frac{R_s}{L_q} T_s & -\omega_r \frac{L_d}{L_q} T_s \\ \omega_r \frac{L_q}{L_d} T_s & 1 - \frac{R_s}{L_d} T_s \end{bmatrix} \quad B_1 = \begin{bmatrix} \frac{T_s}{L_q} & 0 \\ 0 & \frac{T_s}{L_d} \end{bmatrix} \quad (5)$$

$$B_2 = \begin{bmatrix} -\frac{T_s \omega_r}{L_q} & 0 \\ 0 & 0 \end{bmatrix}$$

Even if the machine equations are presented considering L_q and L_d , in the following the motor has been considered without any anisotropy, that means $L_q = L_d = L$.

The equations of the classical Deadbeat control for the PMSM can be obtained from (4) substituting to the $k+1$ currents values the reference ones and solving for the voltages:

$$\begin{bmatrix} V_{qs\ k} \\ V_{ds\ k} \end{bmatrix} = B_1^{-1} \left\{ \begin{bmatrix} i_{qs\ k}^{ref} \\ i_{ds\ k}^{ref} \end{bmatrix} - A \begin{bmatrix} i_{qs\ k} \\ i_{ds\ k} \end{bmatrix} - B_2 \begin{bmatrix} \lambda_m \\ 0 \end{bmatrix} \right\} \quad (6)$$

The resulting control action permits, if no saturation occurs, to reach the current reference value in one sample time. The control voltages obtained are then transformed from the synchronous reference frame to the abc phase coordinates. These signals are finally saturated and injected in a modulator that gives as output the gate signals from the comparison of the control voltages with a triangular waveform carrier of period T_c . Fig. 1 shows the overall control structure.

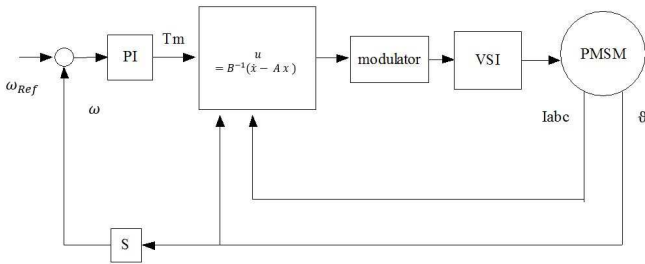


Fig. 1 – Complete control structure

III. OVERSAMPLED DEADBEAT APPROACH

In order to increase the controller sampling time T_x without changing the switching frequency (i.e. the modulator carrier

frequency) some consideration should be done. If the control approach described earlier is simply implemented to a higher frequency, the system becomes quickly unstable as the ratio $\frac{T_x}{T_c}$ decreases due to the interaction with the modulator. The control voltages (6) in fact, are optimal only if they are equal to the inverter output voltages averaged on a T_x period. Using a modulator however, it is guaranteed only on a carrier semi-period, i.e. $\frac{T_c}{2}$. To overcome this problem, at each controller sample time the system computes the optimal control action to reach the current reference at the end of the carrier segment as depicted in Fig. 2. System (6) has been rewritten as

$$\begin{bmatrix} i_{qs\ k+n_c-1} \\ i_{ds\ k+n_c-1} \end{bmatrix} = A_{T_{s_i}} \begin{bmatrix} i_{qs\ k} \\ i_{ds\ k} \end{bmatrix} + B_{1\ T_{s_i}} \begin{bmatrix} V_{qs\ k} \\ V_{ds\ k} \end{bmatrix} + B_{2\ T_{s_i}} \begin{bmatrix} \lambda_m \\ 0 \end{bmatrix} \quad (7)$$

$$i = 0, 1, \dots, n_c - 1$$

where n_c has been defined as 2 times the ratio between the carrier period T_c and the control period T_x . The matrix subscripts indicate the time used in the discretization process and are defined as

$$T_{s_i} = \frac{T_c}{2} - i T_x = (n_c - i) T_x, \quad i = 0, 1, \dots, n_c - 1 \quad (8)$$

i is reset to 0 every $\frac{T_c}{2}$, i.e. at the end of each carrier segment. (7) can then be solved for the control action substituting to the left hand side the current references, resulting in

$$\begin{bmatrix} V_{qs\ k} \\ V_{ds\ k} \end{bmatrix} = B_{1\ T_{s_i}}^{-1} \left\{ \begin{bmatrix} i_{qs\ k}^{ref} \\ i_{ds\ k}^{ref} \end{bmatrix} - A_{T_{s_i}} \begin{bmatrix} i_{qs\ k} \\ i_{ds\ k} \end{bmatrix} - B_{2\ T_{s_i}} \begin{bmatrix} \lambda_m \\ 0 \end{bmatrix} \right\} \quad (9)$$

Please note that the only difference between (6) and (9) is that the latter is computed every T_x with a different set of matrices. Note also that the n_c set of matrices can be precomputed and stored in memory.

If during a carrier semi period the current reference doesn't change, the model parameters are correct and the actual applied voltages match with the computed one, (9) returns a set of n_c equal control action for the whole semi period. In practice however, the voltages calculated are not applied until there is an intersection between one of the phase control voltages and the carrier. This results in a voltage references distortion that can compromise the system performances. A compensation method is proposed in the following to solve this problem.

The machine currents at the time instant k can be written starting from the previous time instant $k-1$ distant T_x as

$$\begin{bmatrix} i_{qs\ k} \\ i_{ds\ k} \end{bmatrix} = A_{T_x} \begin{bmatrix} i_{qs\ k-1} \\ i_{ds\ k-1} \end{bmatrix} + B_{1\ T_x} \begin{bmatrix} V_{qs\ k-1} \\ V_{ds\ k-1} \end{bmatrix} + B_{2\ T_x} \begin{bmatrix} \lambda_m \\ 0 \end{bmatrix} \quad (10)$$

Substituting (10) in (9)

$$\begin{bmatrix} V_{qs_k} \\ V_{ds_k} \end{bmatrix} = B_{1T_{si}}^{-1} \left\{ \begin{bmatrix} i_{qs_k}^{ref} \\ i_{ds_k}^{ref} \end{bmatrix} - A_{T_{si}} \left[A_{T_x} \begin{bmatrix} i_{qs_{k-1}} \\ i_{ds_{k-1}} \end{bmatrix} + B_{1T_x} \begin{bmatrix} V_{qs_{k-1}} \\ V_{ds_{k-1}} \end{bmatrix} + B_{2T_x} \begin{bmatrix} \lambda_m \\ 0 \end{bmatrix} - B_{2T_{si}} \begin{bmatrix} \lambda_m \\ 0 \end{bmatrix} \right\} \quad (11)$$

In order to obtain the compensation term, (11) is written two times. Firstly, equation (11a) is obtained by substituting to $V_{qs_{k-1}}$ and $V_{ds_{k-1}}$ the control voltages calculated by the deadbeat controller equations (9) at the time instant $k-1$ that we will call $V_{qs_{k-1}}^c$ and $V_{ds_{k-1}}^c$.

$$\begin{bmatrix} V_{qs_k}^c \\ V_{ds_k}^c \end{bmatrix} = B_{1T_{si}}^{-1} \left\{ \begin{bmatrix} i_{qs_k}^{ref} \\ i_{ds_k}^{ref} \end{bmatrix} - A_{T_{si}} \left[A_{T_x} \begin{bmatrix} i_{qs_{k-1}} \\ i_{ds_{k-1}} \end{bmatrix} + B_{1T_x} \begin{bmatrix} V_{qs_{k-1}}^c \\ V_{ds_{k-1}}^c \end{bmatrix} + B_{2T_x} \begin{bmatrix} \lambda_m \\ 0 \end{bmatrix} - B_{2T_{si}} \begin{bmatrix} \lambda_m \\ 0 \end{bmatrix} \right\} \quad (11a)$$

Secondly, (11) is written substituting to $V_{qs_{k-1}}^r$ and $V_{ds_{k-1}}^r$ the real voltages applied by the inverter $V_{qs_{k-1}}^r$ and $V_{ds_{k-1}}^r$ obtaining (11b).

$$\begin{bmatrix} V_{qs_k}^r \\ V_{ds_k}^r \end{bmatrix} = B_{1T_{si}}^{-1} \left\{ \begin{bmatrix} i_{qs_k}^{ref} \\ i_{ds_k}^{ref} \end{bmatrix} - A_{T_{si}} \left[A_{T_x} \begin{bmatrix} i_{qs_{k-1}} \\ i_{ds_{k-1}} \end{bmatrix} + B_{1T_x} \begin{bmatrix} V_{qs_{k-1}}^r \\ V_{ds_{k-1}}^r \end{bmatrix} + B_{2T_x} \begin{bmatrix} \lambda_m \\ 0 \end{bmatrix} - B_{2T_{si}} \begin{bmatrix} \lambda_m \\ 0 \end{bmatrix} \right\} \quad (11b)$$

The compensation term permits to obtain $V_{qs_{k-1}}^c$ equal to $V_{qs_{k-1}}^c$ and $V_{ds_{k-1}}^c$ equal to $V_{ds_{k-1}}^c$ hence for the q- and d-axes $comp_{qi}$ and $comp_{di}$ are obtained by subtracting (11b) to (11a) resulting in (12)

$$\begin{aligned} comp_{qi} &= -\frac{1}{L} \left(R_s T_x V_{qs_{k-1}}^r - R_s T_x V_{qs_{k-1}}^c + L T_x \omega_r V_{ds_{k-1}}^r \right. \\ &\quad \left. - L T_x \omega_r V_{ds_{k-1}}^c \right) - \frac{V_{qs_{k-1}}^r - V_{qs_{k-1}}^c}{i-5} \\ comp_{di} &= -\frac{1}{L} \left(R_s T_x V_{ds_{k-1}}^r - R_s T_x V_{ds_{k-1}}^c + L T_x \omega_r V_{qs_{k-1}}^r \right. \\ &\quad \left. - L T_x \omega_r V_{qs_{k-1}}^c \right) \\ &\quad - \frac{V_{ds_{k-1}}^r - V_{ds_{k-1}}^c}{i-5} \end{aligned} \quad (12)$$

The final equation of the oversampled compensated Deadbeat controller are the following:

$$\begin{bmatrix} V_{qs_k} \\ V_{ds_k} \end{bmatrix} = B_{1T_{si}}^{-1} \left\{ \begin{bmatrix} i_{qs_k}^{ref} \\ i_{ds_k}^{ref} \end{bmatrix} - A_{T_{si}} \begin{bmatrix} i_{qs_k} \\ i_{ds_k} \end{bmatrix} - B_{2T_{si}} \begin{bmatrix} \lambda_m \\ 0 \end{bmatrix} + \begin{bmatrix} comp_{qi} \\ comp_{di} \end{bmatrix} \right\} \quad (13)$$

To compute the actual inverter voltages, the previous voltage references are transformed on the abc reference frame, saturated and compared with the modulator carrier. If the phase control voltage is greater or smaller than the carrier for the whole period T_x , the output phase voltage is set equal to $\frac{V_{DC}}{2}$ or $-\frac{V_{DC}}{2}$ respectively. If an intersection between the carrier and the phase voltage is present, the output phase voltage is calculated as the average voltage on the period.

IV. SIMULATION RESULTS

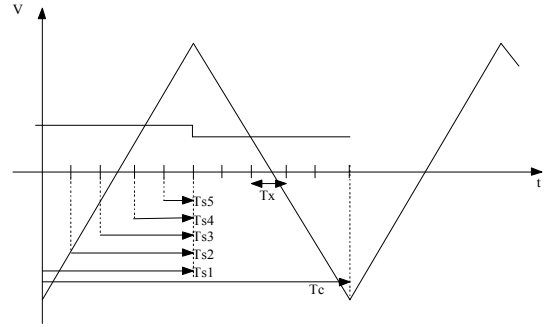


Fig. 2 – Triangular carrier, control voltage for one leg and sample times

The performance of the proposed oversampled Deadbeat algorithm has been tested in simulation using Matlab\Simulink. The system parameters used are listed in Table I. The results included in this paper are obtained implementing the drive with an external speed control loop that generates the reference value for the internal torque control loop. In order to verify the robustness of the proposed system to parameters uncertainties a simulative robustness analysis has been carried out. In a real application both the stator resistance and the inductance can vary. The first one is mainly affected by temperature with an uncertainty up to 30%

TABLE I
SIMULATION PARAMETERS

Name	Description	Value	Unit
R_s	Stator phase resistance	1.5	[Ω]
L	Stator inductance	2.7	[mH]
λ_m	Flux linkage established by magnets	0.06073 3	[V s]
p	Pole pairs	4	-
V_{DC}	DC voltage source	600	[V]
T_c	Carrier period	100	[μ s]
n_c	Oversampling coefficient	5	-
T_x	Control sample time	10	[μ s]

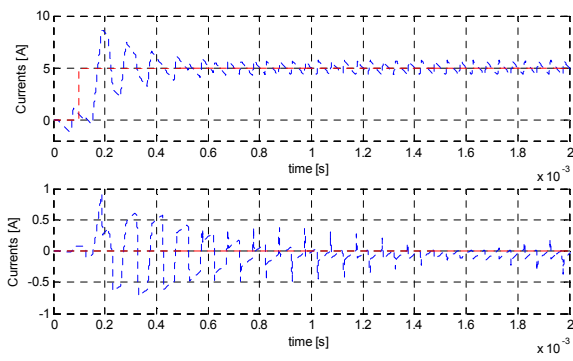


Fig. 3 – Inductance variation of 55%. Left: Classical Deadbeat. Top: I_q (blue) and I_q^{Ref} (red) currents. Bottom: I_d (blue) and I_d^{Ref} (red) currents. Right: Deadbeat Oversampled. Top: I_q (blue) and I_q^{Ref} (red) currents. Bottom: I_d (blue) and I_d^{Ref} (red) currents.

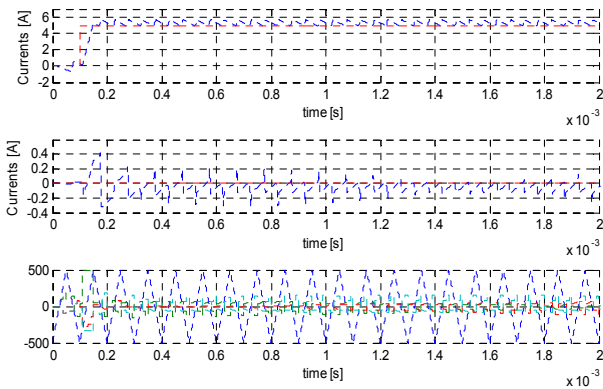
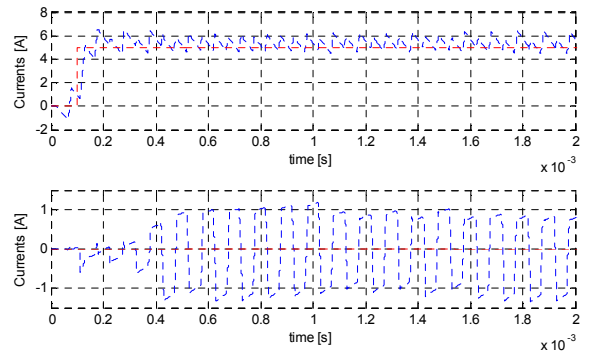


Fig. 4 – Oversample Deadbeat: Top: I_q (blue) and I_q^{Ref} (red) currents. Middle: I_d (blue) and I_d^{Ref} (red) currents. Bottom: triangular carrier and control voltage signals

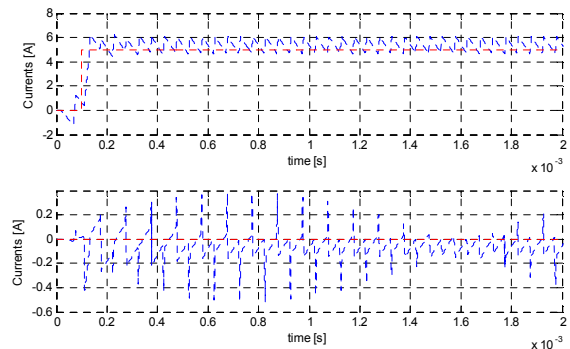


Fig. 6 – Inductance variation of 55%. Oversampled compensated Deadbeat: Top: I_q (blue) and I_q^{Ref} (red) currents. Bottom: I_d (blue) and I_d^{Ref} (red) currents.

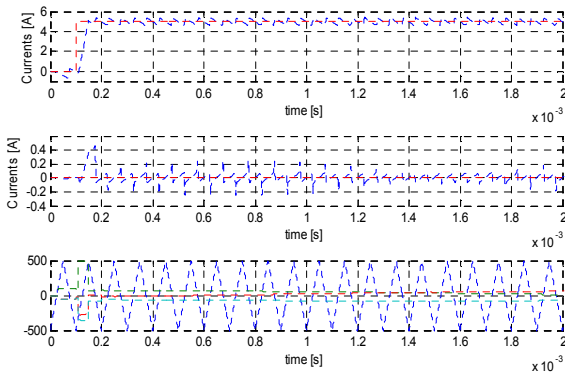


Fig. 5 – Oversampled compensated Deadbeat: Top: I_q (blue) and I_q^{Ref} (red) currents. Middle: I_d (blue) and I_d^{Ref} (red) currents. Bottom: triangular carrier and control voltage signals

while the latter can change due to ferromagnetic saturation. The test, whose results are reported in Fig. 3, has been therefore performed with a reduction of the machine inductance of 55% of the nominal value with respect to the one used in the controller. Fig. 3 consists in a i_q current reference step from 0 to 5 A at 1500 rpm. It shows the

improved dynamic performance of the oversampled Deadbeat (right) compared with the classical Deadbeat (left) achieved in case of an inductance drift. It can be noticed the significant reduction in the initial current transient overshoot. The behaviour without any parameter variation is shown in Fig. 4 and Fig. 5 where the same i_q current transient from 0 to 5 A at 1500rpm is proposed. It can be noticed how the introduction of the oversampling technique creates a distortion in the control voltage signals. This causes a slightly difference in the point of intersection between the carrier and the control voltages resulting in a different time of application of the same inverter configuration; as it can be seen in Fig 4 it leads to a small offset in the controlled i_q and i_d currents. The compensation presented in the previous section has then been implemented and reported in Fig. 5 where the same test condition of Fig 4 is applied. The compensation has the advantage to eliminate the offset in the controlled currents and to remove the distortion of the control voltage signals. Fig 6 shows the case of a reduction of 55% of the nominal inductance with the oversampled compensated deadbeat control approach where a i_q current transient from 0 to 5 A at 1500 rpm is performed. Please notice the absence of overshoot in the response and the only offset is due to the parameter variation. The compensation does not only remove the

controller voltages distortion but also removes the control offset introduced by the oversampling. Moreover it has been observed that comparing the classical Deadbeat (Db), the oversampled Deadbeat (DbOs) and the compensated oversampled Deadbeat (DbOsC) that over 3000 rpm of the rotor mechanical angular speed there is also an increase in performance due to a reduction of the phase currents THD as reported in Table II.

TABLE II
PHASE CURRENT THD [%] FOR DIFFERENT VALUES OF ROTOR SPEED

	3000 rpm	6000 rpm	9000 rpm
Db	7.32	11.3	14.1
DbOs	7.31	12.4	16.7
DbOsC	7.33	11.5	14.8

V. CONCLUSIONS

A new deadbeat current controller implementation is proposed in this work while preserving the main feature of the classical deadbeat control, i.e. that the control action permits, if no saturation occurs, to reach the current reference value in one sample time. The higher controller sampling frequency permits to obtain a more robust solution against parameters variation without increasing the converter switching frequency or compromise steady state performances.

REFERENCES

- [1] Y. A.-R. I. Mohamed and E. F. El-Saadany, "An improved deadbeat current control scheme with a novel adaptive self-tuning load model for a three-phase PWM voltage-source inverter," *IEEE Transactions on Industrial Electronics*, vol. 54, pp. 747-759, 2007.
- [2] S. Mariétoz, A. Domahidi and M. Morari, "High-bandwidth explicit model predictive control of electrical drives", *IEEE Trans. Ind. Appl.*, 2012.
- [3] Z. Ma, S. Saeidi and R. Kennel, "FPGA implementation of model predictive control with constant switching frequency for PMSM drives", *IEEE Trans. Ind. Informat.*, vol. 10, no. 4, pp.2055 -2063, 2014
- [4] H. L.-Huy, K. Slimani, and P. Viarouge, "Analysis and implementation of a real-time predictive current controller for permanent-magnet synchronous servo drives," *IEEE Trans. Ind. Electron.*, vol. 41, no. 1, pp. 110–117, Feb. 1994.
- [5] S. Kouro, P. Cortes, R. Vargas et al., "Model Predictive Control - A Simple and Powerful Method to Control Power Converters," *IEEE Trans. Ind. Electr.*, vol. 56, no. 6, pp. 1826-1838, Jun. 2009.
- [6] J. Rodriguez, M. P. Kazmierkowski, J. R. Espinoza *et al.*, "State of the Art of Finite Control Set Model Predictive Control in Power Electronics," *IEEE Trans. Ind. Inform.*, vol. 9, no. 2, pp. 1003-1016, May 2013.
- [7] A. Formentini, L. de Lillo, M. Marchesoni *et al.*, "A new mains voltage observer for PMSM drives fed by matrix converters," *in EPE*, 2014, pp. 1-10.
- [8] E. Fuentes, D. Kalise, J. Rodriguez *et al.*, "Cascade-Free Predictive Speed Control for Electrical Drives," *IEEE Trans. Ind. Electron.*, vol. 61, no. 5, pp. 2176-2184, 2014.